Geophysical Research Letters

RESEARCH LETTER
10.1029/2019GL082925

Relationship Between the Pacific-North American Pattern and the Frequency of Tropical Cyclones Over the Western North Pacific

Jinjie Song[1,2,3] **and Philip J. Klotzbach**[4]

[1]Key Laboratory of Mesoscale Severe Weather, Ministry of Education, Nanjing, China, [2]School of Atmospheric Sciences, Nanjing University, Nanjing, China, [3]Joint Center for Atmospheric Radar Research, CMA/NJU, Nanjing, China, [4]Department of Atmospheric Science, Colorado State University, Fort Collins, CO, USA

Abstract The frequency of tropical cyclones (TCs) over the western North Pacific during June–November has a significant inverse correlation with the concurrent Pacific-North American (PNA) pattern from 1965 to 2016. During low PNA years, more TCs form north of 12.5°N, with significantly greater TC occurrences from 15 to 20°N, compared to high PNA years. The difference in TC genesis location can be explained by the differences in the genesis potential index derived from the environmental variables in both PNA phases. The PNA influences TC formation primarily by modulating large-scale dynamic conditions, with thermodynamic conditions playing a lesser role. In low PNA years, low-level anomalous cyclonic lows over the Philippines and in the subtropical central Pacific provide significant positive relative vorticity anomalies favorable for TC genesis. Additionally, there is also less vertical wind shear to the north of the Philippines due to enhanced winds at low levels and weaker winds at upper levels.

Plain Language Summary Tropical cyclones (TCs) are the most devastating natural disasters in many coastal regions, including over the western North Pacific (WNP). Therefore, the characteristics and driving mechanisms of WNP TC activity have been studied extensively over the past several decades. Previous publications indicated that El Niño-Southern Oscillation (ENSO) played the most important role on an interannual basis in modulating WNP TC formation, movement, and intensity. However, the interannual frequency of WNP TCs is only weakly influenced by ENSO. Here we find that there exists a significant negative correlation between the annual number of boreal summer WNP TCs and the concurrent Pacific-North American (PNA) pattern. Distinct from other climate modes (e.g., the North Atlantic Oscillation and the Arctic Oscillation), the inverse relationship between WNP TC frequency and the PNA is relatively stable and independent of the period analyzed. Furthermore, the PNA influences the formation of WNP TCs through a modulation of the large-scale environment, particularly the dynamic conditions. During low PNA years, the large-scale dynamic conditions are more favorable for TC development, compared to high PNA years. Our results imply that one may be able to improve the prediction of WNP TC frequency by considering variations in the PNA pattern.

Key Points:
- Boreal summer western North Pacific tropical cyclone frequency is inversely linked to the concurrent Pacific-North American pattern
- A greater number of tropical cyclones form north (south) of 12.5°N during low (high) Pacific-North American pattern phases
- The Pacific-North American pattern influences tropical cyclone genesis predominately by modulating large-scale dynamic conditions

Supporting Information:
- Supporting Information S1

Correspondence to:
J. Song,
songjinjie@nju.edu.cn

Citation:
Song, J., & Klotzbach, P. J. (2019). Relationship between the Pacific-North American pattern and the frequency of tropical cyclones over the western North Pacific. *Geophysical Research Letters*, *46*, 6118–6127. https://doi.org/10.1029/2019GL082925

Received 20 MAR 2019
Accepted 16 MAY 2019
Accepted article online 23 MAY 2019
Published online 10 JUN 2019

1. Introduction

Tropical cyclone (TC) frequency over the western North Pacific (WNP) has exhibited significant temporal variability on different timescales over the past several decades, which is driven primarily by variations in large-scale oceanic and atmospheric patterns (Chan, 2004). Changes in WNP TC numbers have been shown to exhibit significant interannual variability (Chan & Xu, 2009). Several previous publications have investigated the influences of various climate modes on the interannual variation in WNP TC frequency. The occurrence of WNP TCs is very sensitive to both local forcing and remote oceanic forcing represented by different sea surface temperature (SST) patterns, such as the El Niño-Southern Oscillation (ENSO; Chan, 1985; Camargo & Sobel, 2005), the Indian Ocean Dipole (Du et al., 2011; Zhan et al., 2011), the North Pacific Gyre Oscillation (Zhang et al., 2013), the Pacific Meridional Mode (Zhang et al., 2016), and the Atlantic Meridional Mode (Zhang et al., 2017). Although debate continues on the strength of the relationship between WNP TC activity and the stratospheric Quasi-Biennial Oscillation (Camargo & Sobel, 2010; Chan, 1995; Ho et al., 2009), WNP TC frequency is significantly impacted by other different atmospheric circulation patterns, including the North Atlantic Oscillation (NAO; Elsner & Kocher, 2000; Choi & Cha, 2017), the Antarctic Oscillation (Ho et al., 2005), the North Pacific Oscillation (Chen et al., 2015; Wang et al., 2007),

the Arctic Oscillation (AO; Choi & Byun, 2010; Choi et al., 2012), the Pacific-Japan teleconnection pattern (Choi et al., 2010), and the Western Pacific teleconnection pattern (Choi & Moon, 2012).

The impacts of ENSO on WNP TCs have been investigated in many previous studies. El Niño seasons are typically characterized by an eastward and equatorward migration in WNP TC genesis location. WNP TCs forming in El Niño seasons, on average, have a longer duration, reach a greater intensity, and are more likely to recurve than WNP TCs forming in La Niña seasons (Camargo & Sobel, 2005; Chu, 2004). However, there is only a weak correlation between annual total TC numbers over the entire WNP and ENSO (Lander, 1994), despite the statistically significant relationship between the number of intense TCs and ENSO phase caused by the migration in TC formation location and prevailing track (Camargo et al., 2007; Camargo & Sobel, 2005). In addition, Chen et al. (2006) analyzed characteristics of TC activity in different groups categorized by their intensities and found no differences in TC frequency among these groups when stratified by ENSO phase.

By contrast, the frequency of WNP TCs is closely associated with the AO and the NAO, which are the dominant modes of climate variability over the Northern Hemisphere extratropics and the North Atlantic, respectively (Thompson & Wallace, 2000; Wallace & Gutzler, 1981). The AO can significantly influence the interannual variability of WNP TC frequency through modulation of the atmospheric circulation (Choi et al., 2012; Choi & Byun, 2010). More TCs form to the east of 150°E during low AO years than during high AO years (Choi & Byun, 2010). The NAO can change the large-scale flow pattern that consequently then influences WNP TC genesis (Choi & Cha, 2017). For positive and negative NAO years, there are more TC occurrences in the northwestern and southeastern regions of the WNP, respectively (Choi & Cha, 2017). Choi and Cha (2017) further documented a strong positive correlation between the NAO index during June and WNP TC frequency during July and August. However, Zhou and Cui (2014) found that the linkage between WNP TC frequency and the NAO changed from a weak relationship in 1948–1977 to a strong relationship in 1980–2009. Cao et al. (2015) also showed that the strong relationship between WNP TC frequency and the AO during 1968–1986 became weak during 1989–2007. These findings mean that the relationship between WNP TC number and the AO/NAO is unstable and sensitive to the period analyzed.

Although there exists continued debate on the relationship between the NAO and the AO, their patterns are highly correlated (Itoh, 2008). Ambaum et al. (2001) proposed a three-point seesaw system related to the AO, including three centers of action, that is, the Arctic, Euro-Atlantic, and Pacific regions. They argued that the AO is composed of the NAO and the Pacific-North American pattern (PNA), which is one of the most prominent atmospheric modes over the North Pacific (Wallace & Gutzler, 1981). Accordingly, there could be a potential relationship between WNP TC frequency and the PNA. Choi and Moon (2013) found a strong negative correlation between the frequency of TCs influencing Taiwan from June to October and the PNA pattern during the preceding April, which primarily results from the anomalous cyclonic circulation around Taiwan during negative PNA years. This relationship is further considered as an important factor in the formulation of a seasonal prediction scheme for TC frequency near Taiwan (Choi et al., 2014). However, since there is a considerable proportion of WNP TCs occurring outside of the Taiwan region, it is still unknown as to whether the frequency of TCs over the entire WNP is linked to the PNA. Moreover, TCs exhibit different temporal characteristics over different subbasins of the WNP, which is mainly a result of different large-scale environments (Camargo & Sobel, 2005; Chan, 1985). It is also unclear how the PNA modulates TC genesis in other subbasins of the WNP excluding the Taiwan region.

Similar to the AO/NAO, the PNA pattern generally tends to be most pronounced during the boreal winter (Wallace & Gutzler, 1981), which explains why Choi and Moon (2013) and Choi et al. (2014) related the frequency of boreal summer TCs around Taiwan to the PNA pattern in the preceding months. However, L'Heureux et al. (2008) noted that the PNA has an atmospheric presence throughout the entire year, with a wave train in the boreal summer that is shifted poleward of its boreal winter location. Although the impact of the boreal summer PNA on other weather phenomena has been investigated in several publications (L'Heureux et al., 2008; Weng et al., 2007; Wu et al., 2014), the impact of the boreal summer PNA on WNP TC frequency has not been previously discussed. The PNA pattern in boreal summer is somewhat different from that in boreal winter, which mainly features above-average heights to the west of Hawaii and in the southeastern U.S. and below-average heights over the southern Aleutian Islands and over eastern Canada. The above-average heights over the western North America that are apparent in a positive boreal

winter PNA composite are hardly discernible during the boreal summer (Weng et al., 2007). This means that the influence of the boreal summer PNA on WNP TC formation is possibly distinct from the effect of the boreal winter PNA.

It is the goal of this work to explore the interannual variability of the boreal summer TC frequency over the entire WNP as influenced by the concurrent PNA pattern. The manuscript is arranged as follows. Section 2 describes the data and statistical verification methods used in this study. Section 3 outlines a potential relationship between WNP TC formation and the PNA, followed by a discussion of the mechanism of the PNA's influence on WNP TC genesis in section 4. A summary is given in section 5.

2. Data and Methodology

WNP TC best track data between 1965 and 2016 used in this study are from the International Best Track Archive for Climate Stewardship (IBTrACS) v03r10 (Knapp et al., 2010). Only TCs simultaneously recorded by four warning agencies over the WNP, that is, the Joint Typhoon Warning Center, the Japan Meteorological Agency, the China Meteorological Administration, and the Hong Kong Observatory, are considered here, in order to reduce the uncertainty among data sources and enhance the robustness of the results (Song & Klotzbach, 2018). These TCs account for 87, 96, 78, and 89% of the total number of TCs in Joint Typhoon Warning Center, Japan Meteorological Agency, China Meteorological Administration, and Hong Kong Observatory best tracks, respectively. This method also minimizes possible influences of the temporal evolution of observational technologies for weak TCs (e.g., tropical depressions), since stronger TCs are more likely to be identified simultaneously by all four agencies. The TC genesis location refers to the first record that is simultaneously listed by all four agencies, as suggested by Song and Klotzbach (2018). The following results do not change significantly if using the method of identifying the TC formation by the initial position in a TC track. Over the period from 1965 to 2016, approximately 85% of the annual total number of WNP TCs formed during June–November (JJASON). Thus, the present work uses this 6-month period.

Monthly mean SST data are obtained from the National Oceanic and Atmospheric Administration (NOAA) Extended Reconstructed SST v5 over a 2° × 2° grid (Huang et al., 2017). Monthly mean atmospheric data are provided by the National Centers for Environmental Prediction/National Center for Atmospheric Research reanalysis with a horizontal resolution of 2.5° × 2.5° (Kalnay et al., 1996), which are then interpolated to a 2° × 2° grid for calculating the maximum potential intensity (MPI; Emanuel, 1988) and the genesis potential index (GPI; Emanuel & Nolan, 2004). The GPI, as shown by Emanuel and Nolan (2004), is defined as

$$\mathrm{GPI} = \left|10^5\eta\right|^{\frac{3}{2}}\left(\frac{H}{50}\right)^3\left(\frac{\mathrm{MPI}}{70}\right)^3(1+0.1\mathrm{VWS})^{-2}, \quad (1)$$

where η is the absolute vorticity at 850 hPa (in s^{-1}), H is the relative humidity at 600 hPa (in %), VWS is the magnitude of the vertical wind shear between 850 and 200 hPa (in m/s), and the unit of MPI is m/s. Oceanic and atmospheric fields are calculated as seasonal averages over JJASON. JJASON averages of Niño-3.4 SST and the PNA, NAO, and AO indices are provided by NOAA's Earth System Research Laboratory Physical Sciences Division (https://www.esrl.noaa.gov/psd/data/climateindices/). Detailed descriptions of these climate indices and the differences among the AO, NAO, and PNA are provided in the supporting information. Additionally, interpolated Outgoing Longwave Radiation data in NOAA's Climate Diagnosis Center are analyzed here from 1979 to 2016. This excludes missing or inconsistent data before 1979 (Liebmann & Smith, 1996).

The significance levels (p) of the correlation coefficient, the partial correlation coefficient, and the differences in the averages of the two time series are all estimated by Student's t test.

3. Statistical Relationships Between WNP TC Frequency and the PNA

Figure 1a shows an inverse relationship between WNP TC frequency and the PNA during 1965–2016, with a significant correlation coefficient of −0.51 ($p < 0.001$). This means that not only around Taiwan (Choi & Moon, 2013) but also over the entire WNP that TC formation occurs more frequently in negative PNA

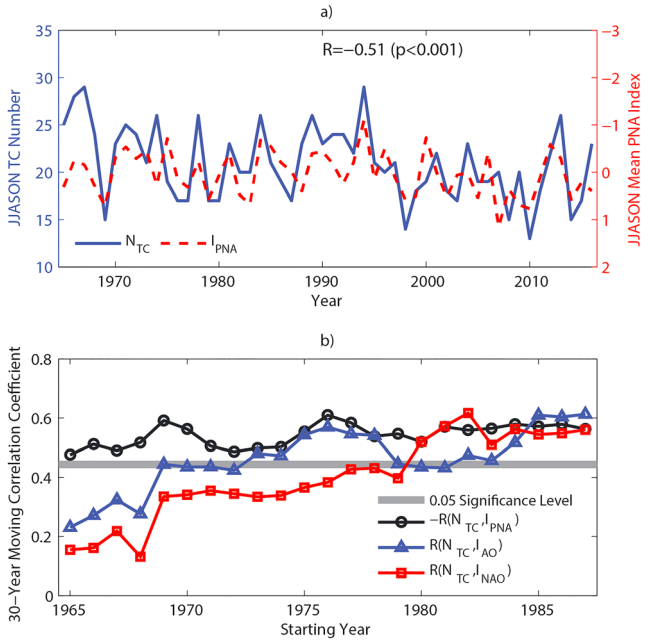

Figure 1. (a) Time series of WNP TC number and the PNA index over the period from 1965 to 2016. (b) Thirty-year moving correlation coefficients between WNP TC number and the PNA (black line), the NAO (red line), and the AO (blue line) from 1965 to 2016.

phases than in positive PNA phases, on average. This inverse relationship is also found between the PNA index and the numbers of TCs with lifetime maximum intensities of tropical storm and typhoon strength, respectively. The correlation coefficients between the PNA index and the numbers of tropical storms (<64 kt) and typhoons (≥64 kt) are −0.28 ($p < 0.05$) and −0.40 ($p < 0.01$), respectively. By contrast, the correlation coefficients of the WNP total TC number versus the NAO and AO indices are 0.36 ($p < 0.01$) and 0.30 ($p < 0.05$) from 1965 to 2016, respectively, which indicates a relatively weaker relationship between these two climate indices than the PNA. Moreover, the partial correlation coefficients between WNP TC frequency and the PNA index are −0.45 ($p < 0.001$) and −0.49 ($p < 0.001$) when the influences of the NAO and the AO are removed, respectively. There is not a significant relationship between WNP TC number and the NAO and AO indices after excluding the PNA effect, with partial correlation coefficients of 0.23 ($p = 0.12$) and 0.12 ($p = 0.39$), respectively. Additionally, the relationship between WNP TC frequency and the PNA index is still significant if the effects of the winter AO and NAO are excluded. Statistically speaking, the variation of WNP TC frequency is independent of the NAO and AO, when the PNA influence is removed.

There is an obvious decadal change in the linkage between WNP TC number and the AO/NAO (Figure 1b). As was found in Zhou and Cui (2014), the weak relationship between the WNP TC frequency and the NAO changes to a strong connection around 1980. There is also an increasing linkage between WNP TC frequency and the AO, with the 30-year correlation coefficient changing from insignificant to significant in the mid-1970s. Note that this result differs from that found in Cao et al. (2015), which may be due to their use of a March–May-averaged AO. By contrast, there is a stable relationship between WNP TC frequency and the PNA from 1965 to 2016, with 30-year correlation coefficients all significant at the 0.05 level (Figure 1b). The stability in the PNA/WNP TC relationship explains why the linkage of the PNA to WNP TC number is much stronger than that of the AO/NAO. In the Northern Hemisphere winter, the AO exhibits more covariability with the North Pacific after 1970 (Overland et al., 1999), while the PNA-NAO coupling shifts from weak to strong in the mid-1970s (Honda et al., 2001). Consequently, it is possible that the connection among the PNA, the NAO, and the AO became stronger in the boreal summer since the 1970s. The aforementioned results indicate that the influence of the AO/NAO on WNP TC frequency mainly derives from their effect linked to the PNA.

Table 1
List of High-PNA and Low-PNA Years During June–November 1965–2016, As Well As the Corresponding TC Frequencies Over the WNP

High PNA		Low PNA	
Year	TC number	Year	TC number
1968	24	1966	28
1969	15	1978	26
1977	17	1981	23
1979	17	1986	19
1983	20	1989	26
1992	24	1990	23
2005	19	1993	22
2008	15	1996	20
2014	15	2012	22
2016	23	2013	26
Mean	18.9	Mean	23.5

Furthermore, in order to compare the spatial difference in the TC formation between different PNA phases, the highest 10 PNA (high-PNA) years and the lowest 10 PNA (low-PNA) years from 1965 to 2016 are first selected based on the JJASON-averaged value of the PNA, after excluding ENSO years (Table 1). El Niño (La Niña) years are defined as the JJASON averages of Niño-3.4 SST anomalies greater (less) than +0.5 °C (−0.5 °C), as has been done in previous studies (Choi & Byun, 2010; Choi & Moon, 2012). The WNP averages 4.6 more TCs in the 10 low-PNA years than in the 10 high-PNA years. This difference is significant at the 0.01 level. Figure 2a further displays the spatial difference in the TC formation location between the two PNA phases. There are more (fewer) TCs forming northward (southward) in the WNP in low-PNA years than in high-PNA years, with a separation in the relationship occurring around 12.5°N. The greatest differences occur over the northern part of the South China Sea) and the WNP east of the Philippines (15–20°N, 110–150°E) where a majority of WNP TCs form (Choi & Byun, 2010). There are also three centers with significant TC genesis differences at around 110–115°E, 130–135°E, and 145–150°E. Surrounding these centers, the TC formation difference

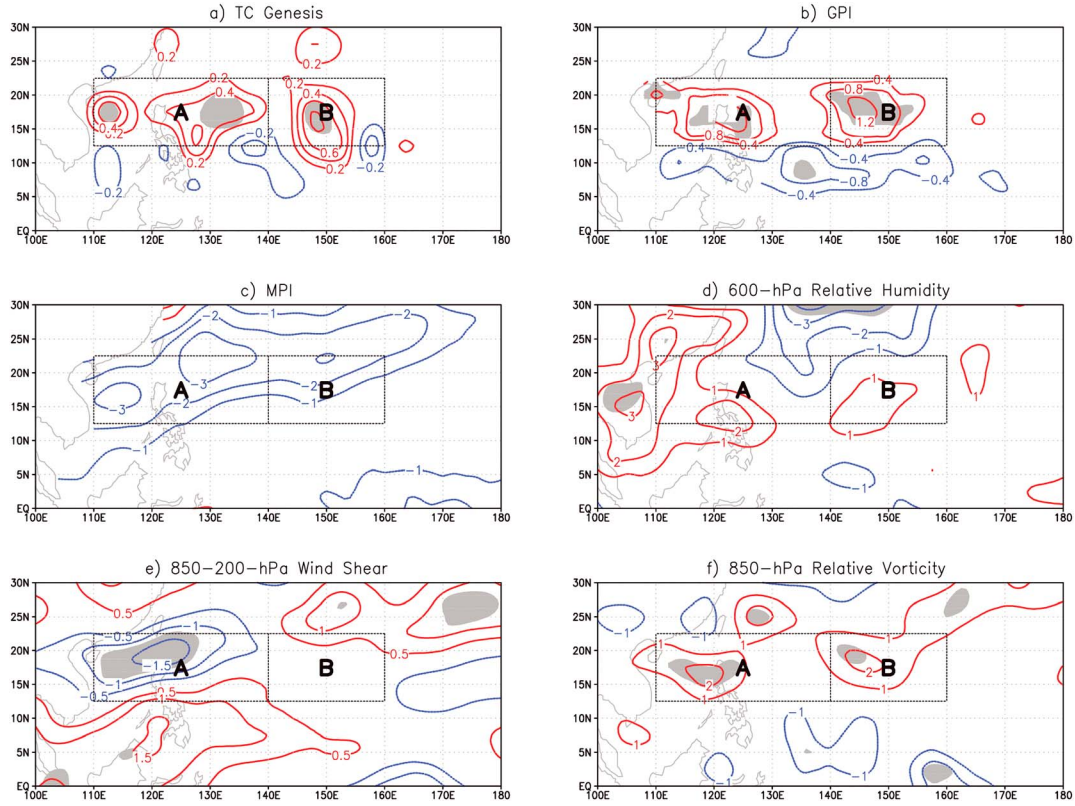

Figure 2. (a) Difference in TC genesis location over the WNP between high-PNA years and low-PNA years in each 5° × 5° latitude-longitude grid area. Shaded regions indicate that the differences are significant at the 0.05 level. (b–f) Differences in the environmental variables between high-PNA years and low-PNA years in each 2° × 2° latitude-longitude grid area for (b) GPI, (c) MPI (m/s), (d) 600-hPa relative humidity (%), (e) 850–200-hPa vertical wind shear (m/s), and (f) 850-hPa relative vorticity (s^{-1}). The resolution is 2° × 2° latitude-longitude in (b, c) and 2.5° × 2.5° latitude-longitude in (d, f). Shaded regions indicate that the differences are significant at the 0.05 level.

is not significant between high-PNA years and low-PNA years. The aforementioned differences still exist when ENSO years are not excluded (Table S1 and Figure S1 in the supporting information).

4. Possible Mechanisms

The GPI (Emanuel & Nolan, 2004), which is a combination of several important environmental variables related to TC development, is applied here to compare the influences of thermodynamic and dynamic factors on TC genesis in different PNA phases. Figure 2b displays the GPI difference between the two PNA phases during JJASON. The spatial distribution agrees well qualitatively with the difference pattern in TC genesis (Figure 2a), implying that the difference in the spatial distribution of WNP TC formation primarily results from different large-scale environments in high-PNA and low-PNA years. The most obvious feature is larger (smaller) GPIs in low-PNA years occurring to the north (south) of 12.5°N than in high-PNA years. There are also three significant centers of the GPI difference located between 15 and 20°N. Compared with Figure 2a, the position of the one center at ~150°E remains consistent, whereas there is a westward migration of the other two center locations. Two regions, A (12.5–17.5°N and 110–140°E) and B (12.5–17.5°N and 140–160°E), are marked in Figure 2 and in the following figures for convenience.

To further examine large-scale environmental conditions responsible for the WNP TC formation modulated by the PNA, the differences in the four variables constituting the GPI are now displayed (Figures 2c–2f). Note that the differences are not significantly changed if the long-term linear trends in these environmental factors are removed. During low-PNA years, lower MPIs occur over almost the entire tropical and subtropical WNP, suppressing TC formation (Figure 2c). The feature of negative MPI differences oriented from southwest to northeast is primarily linked to a similar pattern of negative SST anomalies in low-PNA years (Li et al.,

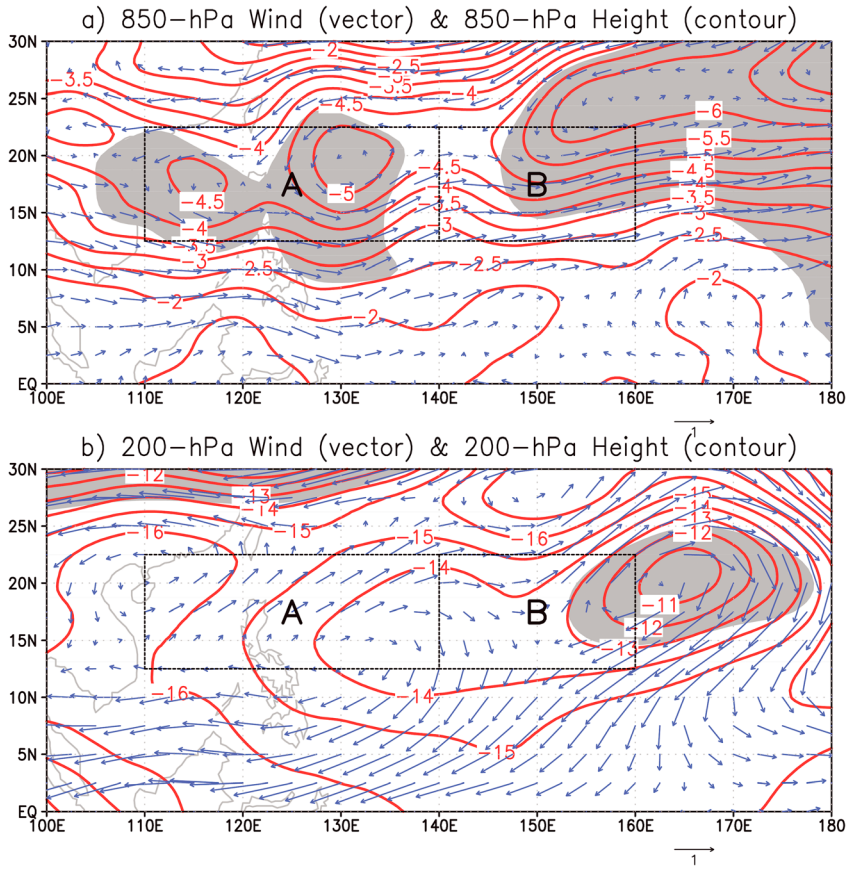

Figure 3. Regressions of horizontal wind (m/s) and geopotential height (gpm) at (a) 850 hPa and (b) 200 hPa, respectively, onto the inverse PNA index in June–November (JJASON) from 1965 to 2016. Shaded regions indicate that the regressions are significant at the 0.05 level.

2018). The midlevel atmosphere in Regions A and B is generally moister during low-PNA years than during high-PNA years, thereby providing more conducive conditions for TC genesis (Figure 2d). Although there are differences in the MPI and 600-hPa relative humidity fields during different PNA phases, these differences are not statistically significant. Consequently, there appears to be only a weak influence of the PNA on WNP TC formation via thermodynamic effects. In addition, there is also an insignificant influence of the PNA on WNP TC genesis via oceanic factors, such as SST and 0–700-m ocean heat content (figure not shown).

The differences in dynamic fields are more significant between different PNA phases (Figures 2e and 2f). More favorable conditions for TC formation are found in most of Region A in low-PNA years, with significantly weaker vertical wind shear and stronger low-level relative vorticity. Region B is only characterized by significantly greater low-level relative vorticity during low-PNA years, whereas the difference in vertical wind shear is small and insignificant between the two PNA phases. In comparison, fewer TC occurrences and the lower GPIs south of 12.5°N (Figures 2a and 2b) are primarily driven by the increased vertical wind shear and reduced low-level relative vorticity (Figures 2e and 2f). To summarize, WNP TC formation is primarily modulated by differences in dynamic conditions between positive and negative PNA years, which is consistent with previous publications indicating the greater importance of dynamic conditions compared with thermodynamic conditions on WNP TC genesis (Chan, 2000; Sharmila & Walsh, 2017).

To further investigate the differences in the large-scale flow pattern during different PNA years, we next regress geopotential height and wind fields at 850 and 200 hPa onto the inverse PNA index (Figure 3). In low-PNA years, there are two anomalous cyclonic lows over the tropical WNP, located near the Philippines and over the subtropical central Pacific, respectively (Figure 3a). Note that this pattern is consistent with the large-scale environmental schematic in the negative PNA phase proposed by Choi and Moon

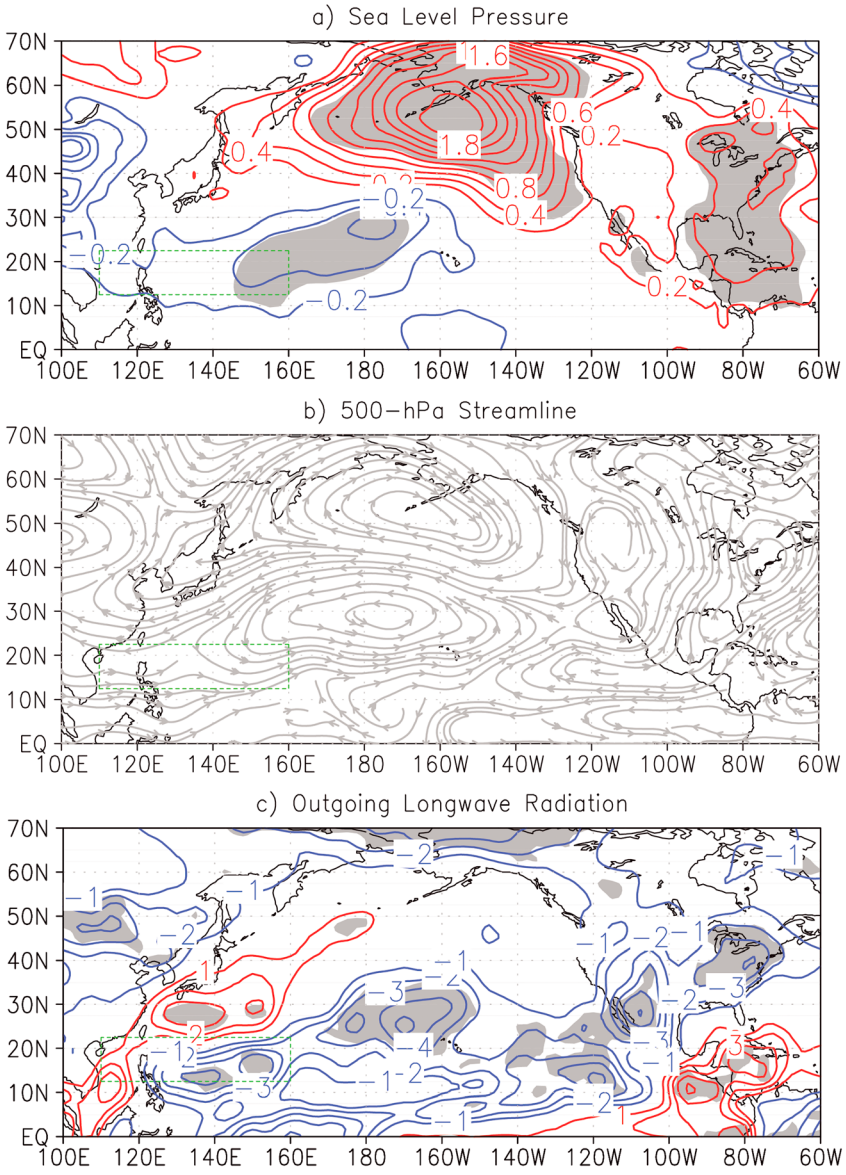

Figure 4. Regressions of (a) sea level pressure (hPa), (b) 500-hPa horizontal wind (m/s) onto the inverse JJASON PNA index from 1965 to 2016, and regressions of (c) outgoing longwave radiation (W/m^2) onto the inverse JJASON PNA index in 1979–2016. Shaded regions in (a) and (c) indicate that the regressions are significant at the 0.05 level.

(2013). Although greater relative vorticity is found in Regions A and B during low-PNA years (Figure 2f), these contributions are not caused by the same processes. The positive relative vorticity anomalies in Region A are linked to the anomalous cyclone near the Philippines, while the positive vorticity anomalies in Region B are associated with the sheared flow in the southwestern part of the low over the central Pacific. On average, there are prevailing southeasterlies at 850 hPa and northeasterlies at 200 hPa over both Regions A and B (Figure S2 in Supporting Information). To the north of the Philippines, the easterlies at 850 hPa and the southwesterlies at 200 hPa (Figure 3) result in enhanced low-level winds and reduced upper level winds, which combined lead to weaker vertical wind shear in Region A during low-PNA years. In contrast, there are, on average, westerlies at both 850 and 200 hPa in Region B, which leads to insignificant changes in vertical wind shear between the two PNA phases.

Figure 4 further investigates how the boreal summer PNA modulates TC formation over the WNP. The negative phase of a boreal summer PNA features below-average sea level pressures to the west of Hawaii and

above-average sea level pressures over the Aleutian Islands and over eastern North America (Figure 4a). At low latitudes, although the anomalous low is centered near the dateline, it does extend westward toward the South China Sea. This anomalous surface cyclone is correlated with cyclonic circulation at low level and midlevel (Figures 3b and 4b), which provides positive vorticity anomalies favorable for tropical convection. There are broad regions of enhanced convection over the tropical WNP, with two significant low centers in Regions A and B (Figure 4c). These anomalously favorable dynamic conditions provide a conducive environment for TC formation over the WNP during low-PNA years.

5. Summary

The influence of the PNA on the formation of TCs over the WNP is investigated in this study. We find a significant inverse relationship between WNP TC number during JJASON and the concurrent PNA phase during the period from 1965 to 2016. The relationship between WNP TC number and the PNA is relatively stable during the ~50-year period examined, which can be considered as the source of the statistical relationship between WNP TC frequency and the AO/NAO that has been documented in previous publications (Choi & Byun, 2010; Choi & Cha, 2017). To examine the reasons for this relationship, the difference of average TC frequency and large-scale conditions between the 10 highest PNA years and 10 lowest PNA years is further analyzed, excluding El Niño and La Niña years. We find that more (fewer) TCs occur to the north (south) of 12.5°N in low-PNA years than in high-PNA years, which is well captured by the increased (decreased) GPI. The significant increase in TC numbers during low-PNA years primarily occurs in two regions: A (12.5–17.5°N, 110–140°E) and B (12.5–17.5°N, 140–160°E).

We document only small differences in MPI and midlevel relative humidity between different PNA phases and consequently find that the PNA influences the genesis of WNP TCs primarily by modulating large-scale dynamical conditions. During low-PNA years, there is an anomalous cyclonic low in the center of Region A, which directly enhances low-level relative vorticity. Meanwhile, low-level easterlies and upper level southwesterlies reduce the vertical wind shear to the north of the low center. Increased low-level relative vorticity and decreased wind shear are both favorable for TC development. In contrast, greater relative vorticity in Region B during low-PNA years is a result of the sheared flow of an anomalous cyclonic low over the subtropical central Pacific. The difference in vertical wind shear in Region B is not significant.

Based on the aforementioned results, we propose that the PNA pattern is a primary contributor to the frequency of WNP TCs. The PNA index, combined with other climate indices, may therefore be applied to develop statistical or statistical-dynamical models for the prediction of WNP TC frequency.

Acknowledgments
This work was jointly funded by the National Key Research and Development Program of China (2018YFC1507305 and 2018YFA0606003) and the National Grand Fundamental Research 973 Program of China (2015CB452800). Klotzbach would like to acknowledge financial support from the G. Unger Vetlesen Foundation. We thank the two anonymous reviewers for very useful comments, which significantly improved the quality of the manuscript. The WNP TC best track data provided by JTWC, JMA, CMA, and HKO are downloaded from ftp://eclipse.ncdc.noaa.gov/pub/ibtracs/v03r10. The National Oceanic and Atmospheric Administration (NOAA) Extended Reconstructed SST v5 data set is available at https://www.esrl.noaa.gov/psd/data/gridded/data.noaa.ersst.v5.html. The National Centers for Environmental Prediction/National Center for Atmospheric Research reanalysis data set is available at https://www.esrl.noaa.gov/psd/data/gridded/data.ncep.reanalysis.html. The AO, NAO, and PNA indices are downloaded from https://www.esrl.noaa.gov/psd/data/climateindices/. The interpolated Outgoing Longwave Radiation (OLR) data in NOAA's Climate Diagnosis Center (CDC) are available at https://www.esrl.noaa.gov/psd/data/gridded/data.olrcdr.interp.html.

References

Ambaum, M. H., Hoskins, B. J., & Stephenson, D. B. (2001). Arctic oscillation or North Atlantic oscillation? *Journal of Climate*, *14*(16), 3495–3507. https://doi.org/10.1175/1520-0442(2001)014<3495:AOONAO>2.0.CO;2

Camargo, S. J., Robertson, A. W., Gaffney, S. J., Smyth, P., & Ghil, M. (2007). Cluster analysis of typhoon tracks. Part II: Large-scale circulation and ENSO. *Journal of Climate*, *20*(14), 3654–3676. https://doi.org/10.1175/JCLI4203.1

Camargo, S. J., & Sobel, A. H. (2005). Western North Pacific tropical cyclone intensity and ENSO. *Journal of Climate*, *18*(15), 2996–3006. https://doi.org/10.1175/JCLI3457.1

Camargo, S. J., & Sobel, A. H. (2010). Revisiting the influence of the quasi-biennial oscillation on tropical cyclone activity. *Journal of Climate*, *23*(21), 5810–5825. https://doi.org/10.1175/2010JCLI3575.1

Cao, X., Chen, S., Chen, G., Chen, W., & Wu, R. (2015). On the weakened relationship between spring Arctic Oscillation and following summer tropical cyclone frequency over the western North Pacific: A comparison between 1968–1986 and 1989–2007. *Advances in Atmospheric Sciences*, *32*(10), 1319–1328. https://doi.org/10.1007/s00376-015-4256-y

Chan, J. C. (1985). Tropical cyclone activity in the northwest Pacific in relation to the El Niño/Southern Oscillation phenomenon. *Monthly Weather Review*, *113*(4), 599–606. https://doi.org/10.1175/1520-0493(1985)113<0599:TCAITN>2.0.CO;2

Chan, J. C. (1995). Tropical cyclone activity in the western North Pacific in relation to the stratospheric quasi-biennial oscillation. *Monthly Weather Review*, *123*(8), 2567–2571. https://doi.org/10.1175/1520-0493(1995)123<2567:TCAITW>2.0.CO;2

Chan, J. C. (2000). Tropical cyclone activity over the western North Pacific associated with El Niño and La Niña events. *Journal of Climate*, *13*(16), 2960–2972. https://doi.org/10.1175/1520-0442(2000)013<2960:TCAOTW>2.0.CO;2

Chan, J. C. (2004). Variations in the activity of tropical cyclones over the western North Pacific. In *Hurricanes and Typhoons: Past, Present, and Future* (pp. 269–296). Hong Kong, China: City University of Hong Kong.

Chan, J. C., & Xu, M. (2009). Inter-annual and inter-decadal variations of landfalling tropical cyclones in East Asia. Part I: Time series analysis. *International Journal of Climatology*, *29*(9), 1285–1293. https://doi.org/10.1002/joc.1782

Chen, D., Wang, H., Liu, J., & Li, G. (2015). Why the spring North Pacific Oscillation is a predictor of typhoon activity over the Western North Pacific. *International Journal of Climatology*, *35*(11), 3353–3361. https://doi.org/10.1002/joc.4213

Chen, T. C., Wang, S. Y., & Yen, M. C. (2006). Interannual variation of the tropical cyclone activity over the western North Pacific. *Journal of Climate*, *19*(21), 5709–5720. https://doi.org/10.1175/JCLI3934.1

Choi, J. W., & Cha, Y. (2017). Possible relationship between NAO and tropical cyclone genesis frequency in the western North Pacific. *Dynamics of Atmospheres and Oceans*, *77*, 64–73. https://doi.org/10.1016/j.dynatmoce.2016.08.006

Choi, K. S., & Byun, H. R. (2010). Possible relationship between western North Pacific tropical cyclone activity and Arctic Oscillation. *Theoretical and Applied Climatology*, *100*(3-4), 261–274. https://doi.org/10.1007/s00704-009-0187-9

Choi, K. S., & Moon, I. J. (2012). Influence of the Western Pacific teleconnection pattern on Western North Pacific tropical cyclone activity. *Dynamics of Atmospheres and Oceans*, *57*, 1–16. https://doi.org/10.1016/j.dynatmoce.2012.04.002

Choi, K. S., & Moon, I. J. (2013). Relationship between the frequency of tropical cyclones in Taiwan and the Pacific/North American pattern. *Dynamics of Atmospheres and Oceans*, *63*, 131–141. https://doi.org/10.1016/j.dynatmoce.2013.05.003

Choi, K. S., Wu, C. C., & Byun, H. R. (2012). Possible connection between summer tropical cyclone frequency and spring Arctic Oscillation over East Asia. *Climate Dynamics*, *38*(11-12), 2613–2629. https://doi.org/10.1007/s00382-011-1088-z

Choi, K. S., Wu, C. C., & Cha, E. J. (2010). Change of tropical cyclone activity by Pacific–Japan teleconnection pattern in the western North Pacific. *Journal of Geophysical Research*, *115*, D19114. https://doi.org/10.1029/2010JD013866

Choi, K. S., Wu, C. C., & Wang, Y. (2014). Seasonal prediction for tropical cyclone frequency around Taiwan using teleconnection patterns. *Theoretical and Applied Climatology*, *116*(3-4), 501–514. https://doi.org/10.1007/s00704-013-0954-5

Chu, P. S. (2004). ENSO and tropical cyclone activity. In *Hurricanes and Typhoons: Past, Present, and Future* (pp. 297–332). New York: Columbia University Press.

Du, Y., Yang, L., & Xie, S. P. (2011). Tropical Indian Ocean influence on northwest Pacific tropical cyclones in summer following strong El Niño. *Journal of Climate*, *24*(1), 315–322. https://doi.org/10.1175/2010JCLI3890.1

Elsner, J. B., & Kocher, B. (2000). Global tropical cyclone activity: A link to the North Atlantic Oscillation. *Geophysical Research Letters*, *27*(1), 129–132. https://doi.org/10.1029/1999GL010893

Emanuel, K., & Nolan, D. S. (2004). Tropical cyclone activity and the global climate system. In *26th Conference on Hurricanes and Tropical Meteorology* (pp. 240–241). Cambridge, MA: MIT.

Emanuel, K. A. (1988). The maximum intensity of hurricanes. *Journal of the Atmospheric Sciences*, *45*(7), 1143–1155. https://doi.org/10.1175/1520-0469(1988)045<1143:TMIOH>2.0.CO;2

Ho, C. H., Kim, H. S., Jeong, J. H., & Son, S. W. (2009). Influence of stratospheric quasi–biennial oscillation on tropical cyclone tracks in the western North Pacific. *Geophysical Research Letters*, *36*, L06702. https://doi.org/10.1029/2009GL037163

Ho, C. H., Kim, J. H., Kim, H. S., Sui, C. H., & Gong, D. Y. (2005). Possible influence of the Antarctic Oscillation on tropical cyclone activity in the western North Pacific. *Journal of Geophysical Research*, *110*, D19104. https://doi.org/10.1029/2005JD005766

Honda, M., Nakamura, H., Ukita, J., Kousaka, I., & Takeuchi, K. (2001). Interannual seesaw between the Aleutian and Icelandic lows. Part I: Seasonal dependence and life cycle. *Journal of Climate*, *14*(6), 1029–1042. https://doi.org/10.1175/1520-0442(2001)014<1029:ISBTAA>2.0.CO;2

Huang, B., Peter W. Thorne, Viva F. Banzon, Tim Boyer, Gennady Chepurin, Jay H. Lawrimore, et al. (2017). NOAA Extended Reconstructed Sea Surface Temperature (ERSST), Version 5. NOAA National Centers for Environmental Information.

Itoh, H. (2008). Reconsideration of the true versus apparent Arctic Oscillation. *Journal of Climate*, *21*(10), 2047–2062. https://doi.org/10.1175/2007JCLI2167.1

Kalnay, E., Kanamitsu, M., Kistler, R., Collins, W., Deaven, D., Gandin, L., et al. (1996). The NCEP/NCAR 40-year reanalysis project. *Bulletin of the American Meteorological Society*, *77*(3), 437–471. https://doi.org/10.1175/1520-0477(1996)077<0437:TNYRP>2.0.CO;2

Knapp, K. R., Kruk, M. C., Levinson, D. H., Diamond, H. J., & Neumann, C. J. (2010). The international best track archive for climate stewardship (IBTrACS) unifying tropical cyclone data. *Bulletin of the American Meteorological Society*, *91*(3), 363–376. https://doi.org/10.1175/2009BAMS2755.1

Lander, M. A. (1994). An exploratory analysis of the relationship between tropical storm formation in the western North Pacific and ENSO. *Monthly Weather Review*, *122*(4), 636–651. https://doi.org/10.1175/1520-0493(1994)122<0636:AEAOTR>2.0.CO;2

L'Heureux, M. L., Kumar, A., Bell, G. D., Halpert, M. S., & Higgins, R. W. (2008). Role of the Pacific–North American (PNA) pattern in the 2007 Arctic sea ice decline. *Geophysical Research Letters*, *35*, L20701. https://doi.org/10.1029/2008GL035205

Li, Y., Tian, W., Xie, F., Wen, Z., Zhang, J., Hu, D., & Han, Y. (2018). The connection between the second leading mode of the winter North Pacific sea surface temperature anomalies and stratospheric sudden warming events. *Climate Dynamics*, *51*(1-2), 581–595. https://doi.org/10.1007/s00382-017-3942-0

Liebmann, B., & Smith, C. A. (1996). Description of a complete (interpolated) outgoing longwave radiation dataset. *Bulletin of the American Meteorological Society*, *77*(6), 1275–1277.

Overland, J. E., Adams, J. M., & Bond, N. A. (1999). Decadal variability of the Aleutian low and its relation to high-latitude circulation. *Journal of Climate*, *12*(5), 1542–1548. https://doi.org/10.1175/1520-0442(1999)012<1542:DVOTAL>2.0.CO;2

Sharmila, S., & Walsh, K. J. E. (2017). Impact of large-scale dynamic versus thermodynamic climate conditions on contrasting tropical cyclone genesis frequency. *Journal of Climate*, *30*(22), 8865–8883. https://doi.org/10.1175/JCLI-D-16-0900.1

Song, J., & Klotzbach, P. J. (2018). What has controlled the poleward migration of annual averaged location of tropical cyclone lifetime maximum intensity over the western North Pacific since 1961? *Geophysical Research Letters*, *45*(2), 1148–1156. https://doi.org/10.1002/2017GL076883

Thompson, D. W., & Wallace, J. M. (2000). Annular modes in the extratropical circulation. Part I: Month-to-month variability. *Journal of Climate*, *13*(5), 1000–1016. https://doi.org/10.1175/1520-0442(2000)013<1000:AMITEC>2.0.CO;2

Wallace, J. M., & Gutzler, D. S. (1981). Teleconnections in the geopotential height field during the Northern Hemisphere winter. *Monthly Weather Review*, *109*(4), 784–812. https://doi.org/10.1175/1520-0493(1981)109<0784:TITGHF>2.0.CO;2

Wang, H., Sun, J., & Fan, K. (2007). Relationships between the North Pacific Oscillation and the typhoon/hurricane frequencies. *Science in China Series D: Earth Sciences*, *50*(9), 1409–1416. https://doi.org/10.1007/s11430-007-0097-6

Weng, H., Ashok, K., Behera, S. K., Rao, S. A., & Yamagata, T. (2007). Impacts of recent El Niño Modoki on dry/wet conditions in the Pacific rim during boreal summer. *Climate Dynamics*, *29*(2-3), 113–129. https://doi.org/10.1007/s00382-007-0234-0

Wu, Z., Chen, S., He, J., & Chen, H. (2014). Quantifications of the Two "Flavours" of El Niño using Upper-Ocean Heat Content. *Atmosphere-Ocean*, *52*(4), 351–362. https://doi.org/10.1080/07055900.2014.942593

Zhan, R., Wang, Y., & Lei, X. (2011). Contributions of ENSO and East Indian Ocean SSTA to the interannual variability of Northwest Pacific tropical cyclone frequency. *Journal of Climate*, *24*(2), 509–521. https://doi.org/10.1175/2010JCLI3808.1

Zhang, W., Leung, Y., & Min, J. (2013). North Pacific Gyre Oscillation and the occurrence of western North Pacific tropical cyclones. *Geophysical Research Letters*, *40*, 5205–5211. https://doi.org/10.1002/grl.50955

Zhang, W., Vecchi, G. A., Murakami, H., Villarini, G., & Jia, L. (2016). The Pacific meridional mode and the occurrence of tropical cyclones in the western North Pacific. *Journal of Climate*, *29*(1), 381–398. https://doi.org/10.1175/JCLI-D-15-0282.1

Zhang, W., Vecchi, G. A., Villarini, G., Murakami, H., Rosati, A., Yang, X., et al. (2017). Modulation of western North Pacific tropical cyclone activity by the Atlantic Meridional Mode. *Climate Dynamics*, *48*(1-2), 631–647. https://doi.org/10.1007/s00382-016-3099-2

Zhou, B., & Cui, X. (2014). Interdecadal change of the linkage between the North Atlantic Oscillation and the tropical cyclone frequency over the western North Pacific. *Science China Earth Sciences*, *57*(9), 2148–2155. https://doi.org/10.1007/s11430-014-4862-z